Using a magnetite/thermoplastic composite in 3D printing of direct replacements for commercially available flow sensors

S J Leigh,[a*] C P Purssell,[a] D R Billson[a] and D A Hutchins[a]

[a] School of Engineering
University of Warwick
Coventry
CV4 7AL
UK

[*] Corresponding Author Email: s.j.leigh@warwick.ac.uk

Abstract

Flow sensing is an essential technique required for a wide range of application environments ranging from liquid dispensing to utility monitoring. A number of different methodologies and deployment strategies have been devised to cover the diverse range of potential application areas. The ability to easily create new bespoke sensors for new applications is therefore of natural interest. Fused deposition modelling is a 3D printing technology based upon the fabrication of 3D structures in a layer-by-layer fashion using extruded strands of molten thermoplastic. The technology was developed in the late 1980's but has only recently come to more wide-scale attention outside of specialist applications and rapid prototyping due to the advent of low-cost 3D printing platforms such as the RepRap. Due to the relatively low-cost of the printers and feedstock materials, these printers are ideal candidates for wide-scale installation as localised manufacturing platforms to quickly produce replacement parts when components fail. One of the current limitations with the technology is the availability of functional printing materials to facilitate production of complex functional 3D objects and devices beyond mere concept prototypes. This paper presents the formulation of a simple magnetite nanoparticle-loaded thermoplastic composite and it's incorporation into a 3D printed flow-sensor in order to mimic the function of a commercially available flow-sensing device. Using the multi-material printing capability of the 3D printer allows a much smaller amount of functional material to be used in comparison to the commercial flow sensor by only placing the material where is specifically required. Analysis of the printed sensor also revealed a much more linear response to increasing flow rate of water showing that 3D printed devices have the potential to at least perform as well as a conventionally produced sensor.

1. Introduction

3D printing is the process of producing physical objects in a bottom-up fashion, directly from computer aided design (CAD) files. Objects are produced through the layer-by-layer deposition of materials in specific patterns that represent a series of cross-sections through an object.[1,2] Once the object has been initially designed in CAD software, a further software package then slices it into a set of 2D cross-sections or 'slices', each representing the component at a specific layer or z-height. The descriptions of the slices that include information about the patterns of the layers and their thickness are then sent to the 3D printer. The layers can be physically constructed in a number of ways depending on the type of 3D printer being used. Powder can be spread onto a tray and then solidified in the required pattern with the application of a liquid binder,[3] by sintering with a laser [4] or by melting with an electron beam.[5] Some machines carry out 3D lithographic processes using light and photosensitive resins [6] and others deposit filaments of molten plastic.[7] Regardless of how each layer is constructed, after the layer is complete the build surface is moved by a fraction of a millimetre and another layer of material is added.

The most prolific technology used in low-cost 3D printers such as the RepRap [8] is Fused Deposition Modeling (FDM) or Fused Filament Modeling (FFM).[9] FFM machines work on the simple principle of extruding a thin (usually < 1 mm) filament of molten thermoplastic (normally from a feedstock of larger filament) through a heated nozzle onto a room temperature or heated build platform to create a filament network.[10] This printed network cools and adheres to the previously deposited layers to build up a solid 3D object. As objects are fabricated in a bottom-up, additive fashion directly from digital designs, with no milling or molding, complex components can be produced with less waste and much more rapidly than through conventional manufacturing technologies that can often require pre-tooling. As such, the technology is highly attractive for the rapid production of replacement engineering parts. However, the current capabilities of low-cost FDM based 3D printers is such that they can, at present, only produce parts using simple engineering plastics, such as Acrylonitrile butadiene styrene (ABS). Therefore, a step-change in the range of available materials is required. The authors have previously reported a procedure to formulate an electrically conductive thermoplastic composite filament for 3D printing of piezoresistive and capacitive sensors.[11] In an effort to expand upon this work it was identified that a material with magnetic properties could be useful for 3D printing of functional devices. In order to demonstrate how a simple composite material of this type could be used to practically carry out a sensing function, production of a flow-sensing device that mimicked the action of a commercially available flow sensor was chosen. The composite material was formulated using the authors' previously reported procedure and used to 3D print the impeller component of the flow sensor. After 3D printing of the sensor, testing not only showed that the functionality was comparable to that of the commercial sensor but the printed sensor exhibited a much more linear response.

2. Flow Sensor Design and Manufacture

2.1 Operating principle of commercially available sensor

Mimicking the function of a commercially available flow device was selected to demonstrate the viability of 3D printing for production of working sensing devices. The device chosen was an electronic flow sensor (RotorFlow® RFO-2500, Gems Sensors Basingstoke, UK). A depiction of the freely available schematic of the flow sensor is presented in figure 1a.[12]
The authors have previously shown that a flow sensor can be produced using Micro-stereolithography (MSL) with a magnetite/acrylate composite material and an Anisotropic magnetoresistive (AMR) sensor to detect rotating magnetic fields.[13] While providing a means for producing such devices with high-resolution and precision, the small build envelope of the MSL instrument limits the size of the devices to miniature flow sensors for applications such as microfluidics and lab-on-a-chip devices.[14] Thus, to produce the selected sensor, an alternative technology is required. A low-cost 3D printing technology such as FFM, where the achievable volume of the printed structures is much larger was identified as a suitable technology. The operating principle of the commercial sensor is as follows. As a liquid passes though the body of the device (figure 1b), it forces a magnetic rotor to rotate with the rate of the rotation is proportional to that of the flow. As the magnetised vanes of the rotor rotate, the moving magnetic fields are detected using a Hall effect sensor that then produces a series of pulses. The frequency of the pulses is proportional to the rate of flow of the liquid passing through the sensor. Hall effect sensors are commonly used in applications such as this for measuring the speed of rotating shafts or wheels.

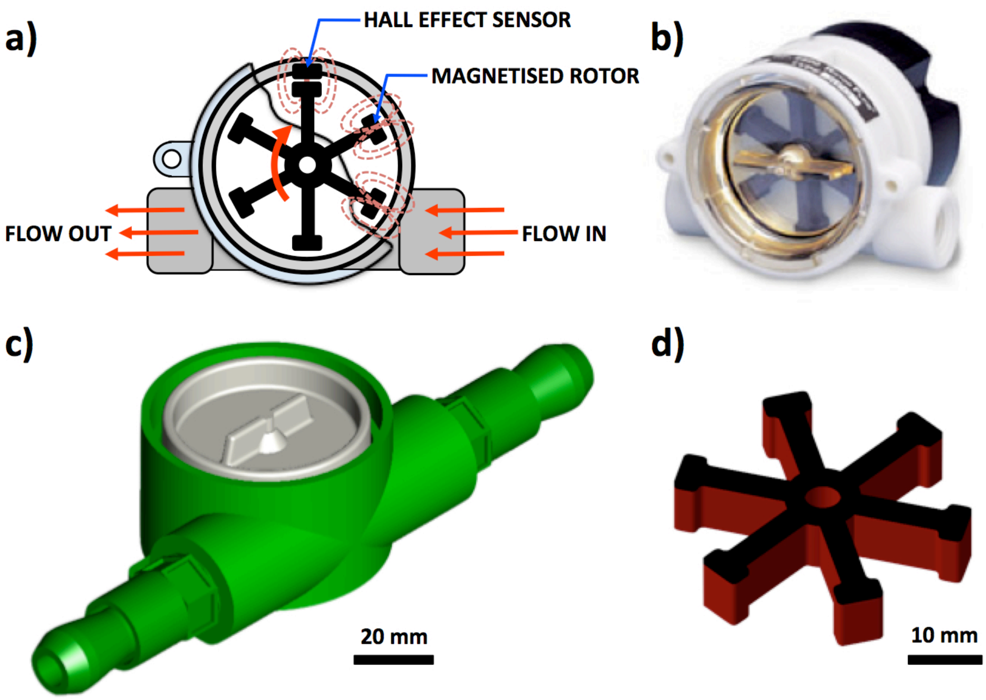

Figure 1 a) Schematic detailing the operation of a commercially available flow sensor, b) picture of commercially available flow sensor, c) CAD design of 3D printable sensor and d) CAD design of 3D printable central impeller.

2.2 Design of 3D printed flow sensor

Taking the commercial RotorFlow® sensor as inspiration, in CAD software (Solidworks, Dassault Systèmes, France) a sensor with the same footprint that could be produced using a standard off-the-shelf FDM 3D printer was designed. The design of the sensor is presented in figure 1c and the design of the printed impeller is presented in figure 1d. In contrast to fabricating the complete impeller from a ferrous material as with the commercial sensor, it was decided to use the multi-material capability of the 3D printing system to print the main body of the impeller from the standard ABS print material and then print a small portion of formulated magnetite composite on the top surface of the impeller. This would serve two purposes: to use the mechanical properties of the ABS to maintain the structural integrity of the impeller, especially at high flow rates and secondly, to demonstrate that if placed optimally, only a small portion of a functional material is needed to achieve a functional effect.

In the commercially available sensor, the impeller is entirely composed of a ferrous material (an approximate volume of 3908.45 mm^3). In the 3D printed sensor, it was surmised that only a small fraction of the impeller would be required to be composed of ferrous material for the sensor to operate. Thus, the printed composite region was selected to be equivalent to two printed 0.250 mm layers from a total impeller height of 9.25 mm. This reduction in the required volume of functional material would also demonstrate that 3D printing would be the ideal technology to consider when the availability (due to cost or scarcity) of functional raw materials may be at a premium.

2.3 Composite material formulation

In order to produce the impeller on the 3D printer a simple magnetite thermoplastic composite was devised. The material was formulated as per the authors' previously reported procedure for producing composite feedstock materials for FFM research.[11] Briefly, magnetite particles (<50 nm nominal diameter, Sigma-aldrich, UK) were stirred in dichloromethane (DCM) while the commercial polycaprolactone formulation (Polymorph, Rapid Electronics, UK) was added. The resulting solution was stirred for 1 hour, then the solvent allowed to evaporate at room temperature and pressure. This simple process yielded a composite polymer film that could be reheated in a water bath and rolled between two glass plates to provide a 3 mm rod of material as a feedstock for the 3D printer.

2.4 Flow sensor production

Production of the flow sensor was carried out using a Bits from Bytes BFB3000 3D printer. In order to create a print file for the BFB printer, the CAD file (in .stl format) was transferred into the Axon 2 software supplied with the printer. Production of the complete device, including the main body took approximately 4 hours in total. The print settings for standard polylactic acid (PLA) filament were selected when printing the magnetite composite. A picture of the completed device and a macro picture of the impeller are presented in Figure 2c and figure 2d respectively. The two printed layers of darker material can clearly be seen on the upper surface of the printed impeller.

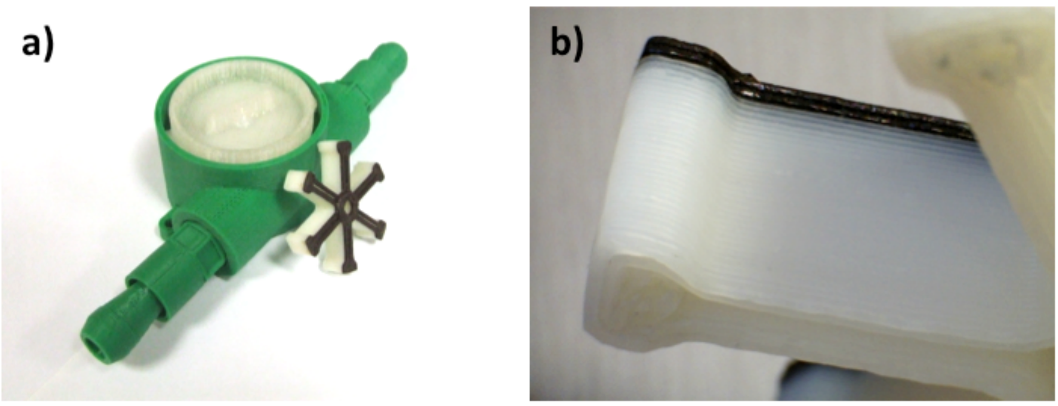

Figure 2 a) photograph of the printed flow sensor and impeller and b) macro image of the printed impeller showing the interface between the formulated composite and the ABS material.

In order to measure the rotation of the 3D printed impeller within the sensor, a Honeywell HMC1001 AMR sensor was used in place of the Hall effect sensor utilised in the commercial flow sensor. The AMR sensor and associated circuit was employed to detect the magnetic fluctuation of the rotating impeller such that the frequency of rotation could be observed and measured on an oscilloscope .

3. Composite Material Analysis

Prior to incorporation in the composite, a portion of the as-received magnetite particles was transferred to carbon tape and imaged using Scanning electron microscopy (SEM). The SEM image is presented in figure 2a. As can be seen from the SEM image, while the particles have quoted nominal diameter of < 50 nm, due to the magnetic-interaction-induced aggregation of the particles they exist as much larger (~ 6 um to ~ 120 um) clusters of smaller particles. This behavior is common in magnetite-containing fluids.[15]

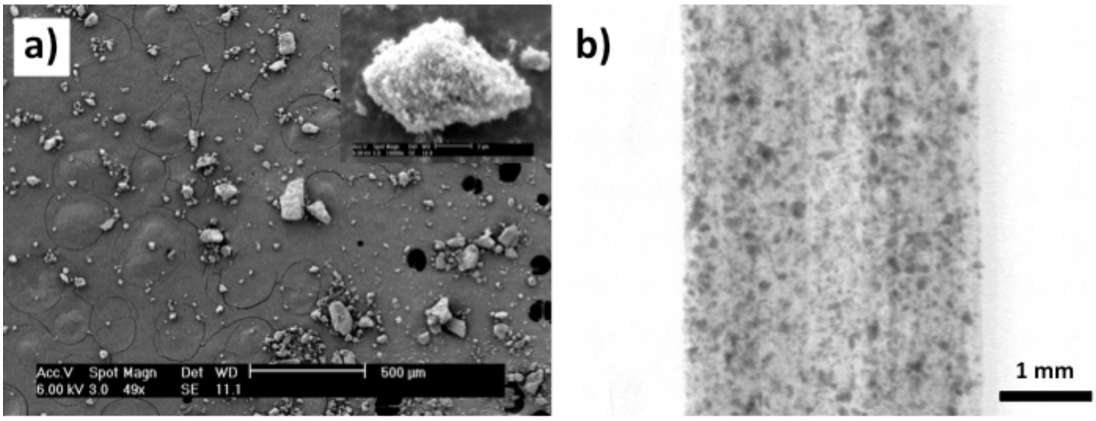

Figure 3 a) SEM image of the as-received magnetite nanoparticles on the surface of a section of carbon tape and b) X-ray image of a section of the printed composite showing the dispersion of magnetite (darker regions) in the polymer matrix.

After formulation of the composite into a 3 mm filament rod, a back-scattered electron (BSE) SEM image of a cut face was taken. The BSE imaging confirmed that although some particle aggregates were still present, the magnetite filler was evenly distributed through the polymer matrix and not confined to the edges or core of the rod. In order to understand the effect of 3D printing on the material itself, a section of a magnetite impeller arm was imaged through it's upper surface using the 2D imaging capability of a micro focus X-ray CT scanner (Skyscan 1174, Bruker). The image (taken at a source voltage of 50kV and scan pixel size of 11.48 μm) is presented in figure 3b. The x-ray imaging revealed that after passing through the print nozzle, the magnetite particles (darker regions in images) remained dispersed through the polymer matrix with no apparent negative effects, such as particle removal or spatial confinement. The darkness (density) of the matrix surrounding the larger aggregates also alludes to the presence of smaller particles or aggregates (beyond the instrument imaging resolution) being dispersed in the polymer matrix. A potential route to improving the dispersion of particles and reducing the occurrence of larger particle aggregates could be to directly synthesise polymer or surfactant stabilised particles for incorporation into the polymer matrix, however the potential impact on sensor functionality is at present unknown.

4. Flow Sensor Testing

In order to test the functionality of the printed sensor compared to the commercially available sensor, the printed sensor was tested using a combination of both compressed air and water.

The initial test of the 3D printed sensor was carried out using air flow from a compressed air system. The aim if this test was to first establish the stability of readings obtained from the sensor. It might be hypothesised that due to the thermoplastic construction of the sensor, if exposed to sustained use, any friction might cause the structure to heat up and deform, thus having a negative impact on its sensing capability. Air was chosen as the flowing phase in this case as the presence of the liquid instead might serve to lubricate any contact and reduce friction. A representative plot of measured frequency versus time for a period of 120 secs is presented in figure 4a. For the presented data, the mean measured value (red horizontal line on graph) was 40.8 Hz with a standard deviation of 1.2 Hz. Beyond the excerpt shown, this level of stability from the sensor was seen to extend over much larger time periods and suggests that the printed sensor is capable of operating with a reasonable degree of accuracy.

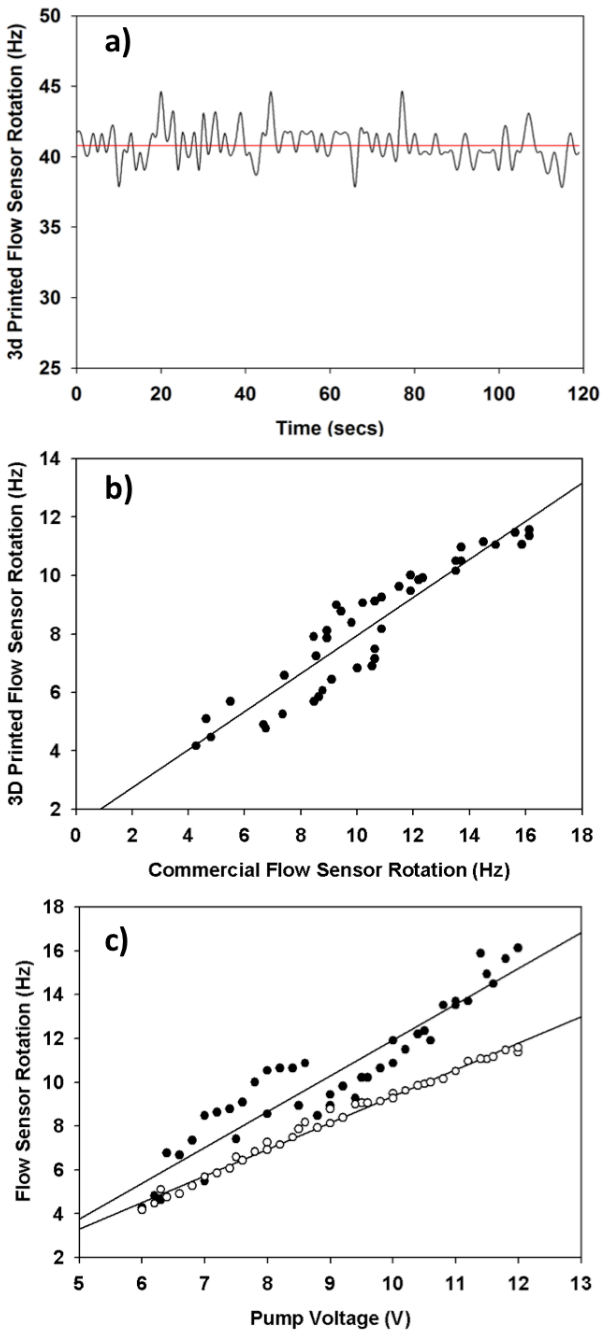

Figure 4. Graphs showing a) stability of measured rotation of sensor under constant air flow (red horizontal line indicates mean value), b) correlation between the commercially available flow sensor when exposed to water flow and c) response of the commercial sensor (*black dots*) and 3D printed sensor (*white dots*) to increasing water flow rate (expressed in terms of pump voltage).

A second test was carried out by connecting both sensors to a recirculating pumped water system (DC15/5 Centrifugal Pump, Totton Pumps, UK) and the frequency correlation of the sensors recorded and plotted (figure 4b). It can be seen that the correlation between the two sensors was approximately linear with the 3D printed sensor displaying an average difference of ± 2.2 Hz from the commercial sensor. The results of the previous stability test indicate that inherent fluctuations in the measured frequency could potentially contribute to any recorded deviations from the linear behavior.

In order to fully characterise the performance of the printed sensor, the rotation speed of each sensor was recorded against increasing pump voltage (and hence increasing flow rate) in the recirculating water system (figure 4c). The readings from each sensor were recorded using identical oscilloscope signal averaging. Surprisingly, the 3D printed sensor exhibited a much more linear response to flow rate compared to the commercial sensor. The reasons for this difference are still unclear but could arise from operating the commercial sensor outside it's optimum calibrated range. The ability of the printed sensor to yield such a linear response further supports that any error in its measured values alone arises from the inherent stability of the sensor and can thus be accounted for.

It is noteworthy that after the sensor tests there was no obvious separation of the magnetite composite layers from the underlying ABS layers of the impeller, indicating good interfacial adhesion. It can be hypothesised that this is due to the mechanical interlocking of the two discrete materials, where the composite is printed at a lower temperature than the ABS, allowing it to interlock into the surface topology of the ABS filament network. This interface stability is encouraging when considering such printed devices for applications where use of a conventional two-shot injection molding approach might require an additional adhesive to achieve a strong bond between materials. This demonstration of the robustness of 3D printed flow sensors while exhibiting a linear response over such a large range of flow rates and conditions is a very encouraging step towards the use of 3D printing for commercial manufacture of functional sensors.

3. Conclusions

By formulating and 3D printing with a functional material based on the incorporation of magnetite particles, the ability to take a commercially available flow sensor and mimic it's operation in a working 3D printed device has been demonstrated. As an advantage, the 3D printed sensors not only use a versatile circuit that can be reused when a new shape/structured device is required and produced but also only use a small amount of material in order to achieve the same function as the commercial flow sensor. Furthermore, when compared to the commercial sensor, the flow sensor exhibits highly encouraging performance in terms of the linearity of its response with predictable accuracy. This work demonstrates that far from being solely a prototyping technology, 3D printing is viable technology for production of devices and products beyond mere concept prototypes.

4. Acknowledgements

This work was part funded by the EPSRC UK Research Centre In Nondestructive Evaluation (RCNDE). The authors would also like to thank Mr Martin Davis (University of Warwick, School of Engineering) for assistance with SEM imaging.

5. References

1. Murr L E, Gaytan S M, Ramirez D A, Martinez E, Hernandez J, Amato K N, Shindo P W, Medina F R and Wicker R B 2012 Metal Fabrication by Additive Manufacturing Using Laser and Electron Beam Melting Technologies *J. Mater. Sci. Technol* **28** 1-14

2. Melchels F P W, Domingos M A N, Klein T J, Malda J, Bartolo P J and Hutmacher D W 2012 Additive manufacturing of tissues and organs *Prog. Polym. Sci* **37** 1079-1104,

3. Khalyfa A, Vogt S, Weisser J, Grimm G, Rechtenbach A, Meyer W and Schnabelrauch M 2007 Development of a new calcium phosphate powder-binder system for the 3D printing of patient specific implants *J Mater Sci Mater Med* **18** 909-916

4. C Dai, H H Zhu, L D Ke, W J Lei and B J Chen 2011 Development a Cu-based Metal Powder for Selective Laser Micro Sintering *J. Phys.: Conf. Ser.* **276** 012016

5. J Parthasarathy, B Starly, S Raman, A Christensen 2010 Mechanical evaluation of porous titanium (Ti6Al4V) structures with electron beam melting (EBM) *J Mech Behav Biomed Mater* **3** 249-59.

6. V Chan, P Zorlutuna, J H Jeong, H Kong, R Bashir 2010 Three-dimensional photopatterning of hydrogels using stereolithography for long-term cell encapsulation *Lab Chip* **10** 2062-2070.

7. D Drummer, S Cifuentes-Cuéllar, D Rietzel 2012 Suitability of PLA/TCP for fused deposition modeling *Rapid Prototyping Journal* **18** 500-507.

8. J M Pearce 2012 Building Research Equipment with Free, Open-Source Hardware *Science* **337** 1303.

9. X Yan, P Gu 1996 A review of rapid prototyping technologies and systems *Computer-Aided Design* **28** 307-318.

10. Y-J Seol, T-Y Kang, D-W Cho 2012 Solid freeform fabrication technology applied to tissue engineering with various biomaterials *Soft Matter* **8** 1730-1735.

11. S J Leigh, R J Bradley, C P Purssell, D R Billson, D A Hutchins 2012 A simple, low-cost conductive composite material for 3D printing of electronic sensors *PLoS ONE* **7** e49365.

12. -available at http://www.gemssensors.com/CustomerSupport-CN/Literature-pdfs/Operating-Principle-Installation-and-Maintenance/RotorFlow-Operating-Principle.

13. S J Leigh, C P Purssell, J Bowen, D A Hutchins, J A Covington, D R Billson 2011 A miniature flow sensor fabricated by micro-stereolithography employing a magnetite/acrylic nanocomposite resin *Sensors and Actuators A: Physical* **168** 66-71.

14. A S Nezhad, M Ghanbari, C G Agudelo, M Packirisamy, R B Bhat, A Geitmann 2013 PDMS Microcantilever-Based Flow Sensor Integration for Lab-on-a-Chip *Sensors Journal* **13** 601-609.

15. W. Jiang and L. Wang 2010 Monodisperse magnetite nanofluids: Synthesis, aggregation, and thermal conductivity *J Appl Phys* **108** 114311.